Title: Design and CFD-based Performance Verification of a Family of Low-Lift Airfoils

Presenting author: Panagiotis K. Chaviaropoulos[1] (tchaviar@fluid.mech.ntua.gr)

Co-authors: Giorgos Sieros[2] (gsieros@cres.gr)
John Prospathopoulos[1] (jprosp@fluid.mech.ntua.gr)
Kostantinos Diakakis[1] (diak@fluid.mech.ntua.gr)
Spyros Voutsinas[1] (spyros@fluid.mech.ntua.gr)

1 : NTUA, 9 Heroon Polytechniou, 15780, Zografou, Athens, GREECE
2 : CRES, 19th km Marathonos Ave., 19009, Pikermi, GREECE

1. Introduction

In the framework of INNWIND.EU FP7 Project CRES and NTUA investigate the potential of low-induction rotors (LIR) in improving the energy yield of large offshore turbines and reducing the cost of electricity produced. As discussed in [1] and [2] the best way to implement the LIR concept is by using low-lift airfoils, e.g. airfoils having their maximum $k = C_L/C_D$ at moderate C_{LDES}(design C_L)values. It is not easy, however, to get a high performance, thick enough, airfoil with k values 100+, which is a normal achievement for the high lift airfoil families. This difficulty is increasing as C_{LDES} gets smaller. The design and performance verification, with state of the art CFD, of a family of low lift profiles aiming to operate in the range or Reynolds and Mach numbers corresponding to a 10MW LIR is the scope of the present work.

2. Approach

Table 1 shows the operating conditions at different blade sections of a LIR version of the 10MW Reference Wind Turbine of INNWIND.EU. The relative thickness of the airfoils along the original blade span varies from 60% in the near-root section to 21% at the tip. Next to the relative thickness we present the Reynolds and Mach number at rated conditions as well as their minimum value within the turbine operating envelope. Since the same airfoil is used at different spanwise positions there are multiple rows in the table sharing the same thickness. From those we use the highlighted rows to specify our design conditions.

Table 1: Intended thickness and operating conditions

Section Thickness	Re (rated)	Ma (rated)	Re (Min)	Ma (Min)
60.00%	**7.0×10^6**	**0.05**	4.4×10^6	0.03
40.10%	**11.0×10^6**	**0.07**	7.0×10^6	0.05
35.00%	**14.0×10^6**	**0.09**	9.0×10^6	0.06
30.00%	**17.0×10^6**	**0.12**	10.0×10^6	0.07
24.00%	**20.0×10^6**	**0.16**	12.0×10^6	0.10
24.00%	**16.0×10^6**	**0.25**	11.0×10^6	0.15
24.00%	**13.0×10^6**	**0.30**	8.0×10^6	0.18
21.00%	**20.0×10^6**	**0.16**	12.0×10^6	0.10
21.00%	**16.0×10^6**	**0.25**	11.0×10^6	0.15
21.00%	**13.0×10^6**	**0.30**	8.0×10^6	0.18
18.00%	**16.0×10^6**	**0.25**	11.0×10^6	0.15
15.00%	**16.0×10^6**	**0.25**	11.0×10^6	0.15

The airfoils are parametrized using Bezier curves with 9-12 control points for representing the complete shape in one piece. The objective function of the design is the maximization of the airfoil performance (lift over drag) within a desired rangeof lift coefficients. The optimizer used employs a combination of evolutionary [3] and gradient-free [4] methods. The direct solver used for the calculation of the objective function is XFOIL [5].

Once the airfoil shapes are obtained their performance is verified using the available airfoil analysis toolkit of NTUA comprising, besides XFOIL, the compressible CFD code MaPFlow [6] and the strong viscous-inviscid interaction code Foil2w [7]. Transitional calculations with MaPFlow have been performed for both fixed transition (transition points derived from X with the e^N method) but also for free transition using the Schlichting-Polhausen method [8].

3. Main body of abstract

Following our earlier conclusions of [1] the low lift airfoils shall be designed for C_{LDES}=0.8, instead of C_{LDES}=1.2 to1.3 which is the normal range for high lift profiles. To avoid deep minima (a highly optimized objective function which rapidly deteriorates when the design variables are slightly perturbed) that characterize single point designs, we designed the airfoils for a maximum mean performance within a range of design lift coefficients C_{LDES}=[0.7 to 0.9] instead of using the single C_{LDES} =0.8 value.

The design objective is therefore stated as:

$$Maximize \left[\int_{C_{LDES1}}^{C_{LDES1}} \left\{W_l \left(\frac{C_L}{C_D}\right)_l + W_t \left(\frac{C_L}{C_D}\right)_t\right\} dC_L\right], W_l + W_t = 1$$

where [C_{LDES1}, C_{LDES2}] is the range of the design lift coefficient, centered around the actual design point and W_l , W_t are the laminar / turbulent flow weights.

An important issue for the design specifications is the way one handles transition. We are referring to designs at very high Reynolds numbers and, therefore, a back-loaded laminar airfoil may perform significantly better than a front-loaded one which better suits fully turbulent flows. On the other hand it is known that the performance of laminar airfoils may become very poor when the flow is tripped to turbulent. But even if a good part of laminar flow exists over the airfoil it is quite uncertain how the high turbulence content of the atmospheric boundary layer will influence the transition location through the bypass mechanism. To ensure some conservatism in our designs we shall optimize the airfoil shapes for their weighted transitional / fully turbulent performance.

Following the design specifications of Table 1 we produced low-lift profiles with relative thicknesses 15%, 18%, 21%, 24%, 30% and 40%. With the exception of the two ending family members (15% and 40%) where a single low-lift airfoil was designed, we generated for all other thicknesses two low-lift profiles of different laminar / turbulent flow weighting. The laminar / turbulent weighting was set to 30%-70% (denoted as 30-70 from this point on) for the first low-lift family (not shown here) and to 10-90 (or 20-80 for the thicker members) for the second family. FIGURE 1 presents the10-90/20-80 low-lift family.

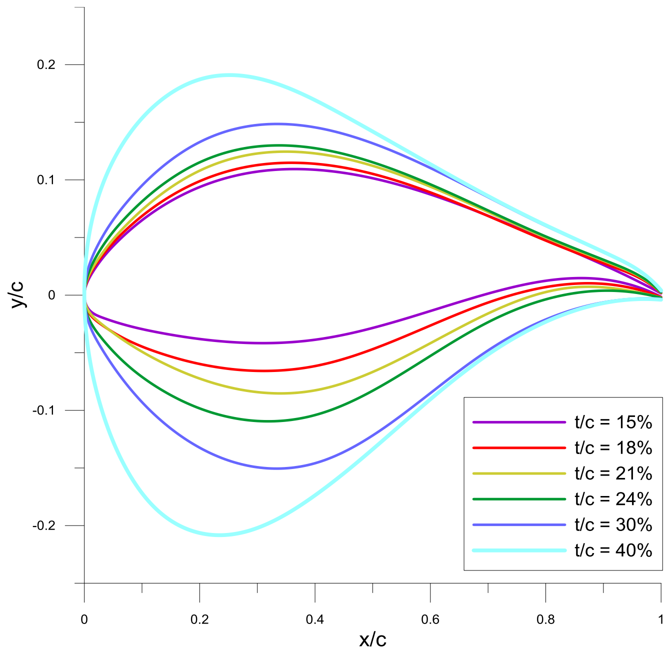

FIGURE 1: The 10-90/20-80 family of Low Lift profiles

Some preliminary simulations using XFOIL show that the 30-70 family is performing slightly worse than the "more conservative" 10-90/20-80 at fully turbulent conditions (FIGURE 2). On the other hand, the 30-70 family is performing better (some members like the 21% and 24% much better) that the 10-90 when the flow is transitional (FIGURE 3). For the transitional flow calculations, the e^N transition model with N=4 is implemented.

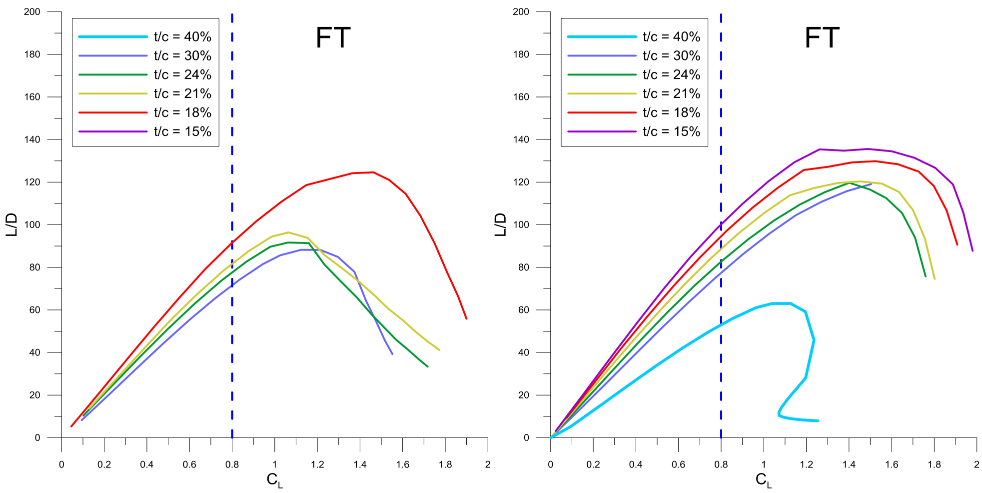

FIGURE 2 Performance (L/D) of the Low Lift family profiles at fully turbulent flow conditions. Left the 30-70 and right the $1_{(2)}0$-$9_{(8)}0$ designs

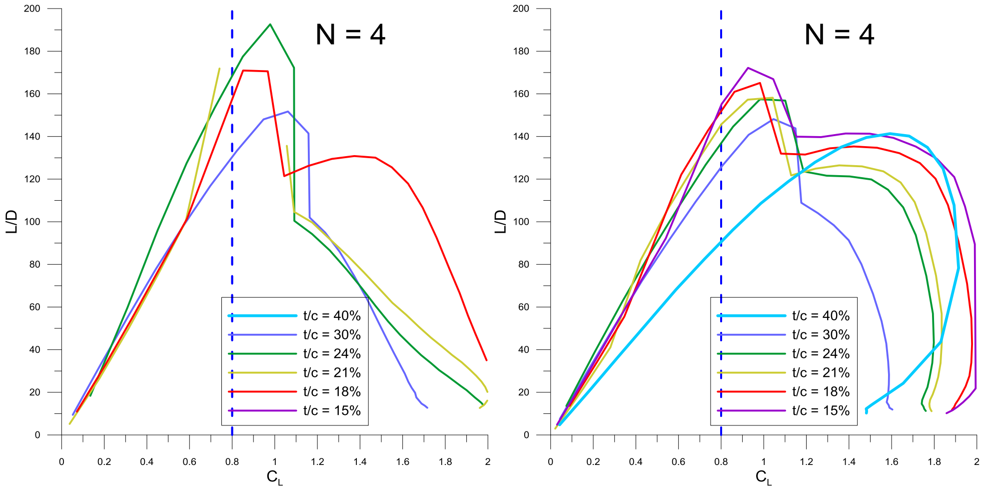

FIGURE 3: Performance (L/D) of the Low Lift family profiles at transitional flow conditions. Left the 30-70 and right the $1_{(2)}0$-$9_{(8)}0$ designs

The 10-90/20-80 family looks more consistent, both geometrically (location of maximum thickness) and performance wise (changing monotonically with the thickness), than the 30-70 one. For these reasons and for introducing some conservatism to the possible energy capture gains of the low induction rotor analysis, the analysis proceeded with the 10-90/20-80 choice.

As a next step, the performance of the 10-90/20-80 choice is further evaluated with the MaPFlow compressible Navier-Stokes solver and the Foil2w viscous-inviscid interaction solver. Both MaPFlow and Foil2w simulations are performed at fully turbulent and fixed transition flow conditions using the transition locations predicted by XFOIL. Furthermore, MaPFlow simulations are also performed for free transitional flow using the Schlichting-Polhausen transition model. In FIGURE 4 and FIGURE 5 the performance (L/D) results for the 18% and 24% are presented. At transitional flow conditions, all models predict considerably high values around the design point C_{LDES}=0.8, ranging between 135 and 150 for the 18% airfoil. As thickness increases to 24%, performance is reduced, ranging between 125 and 135. MaPFlow predictions using the Sclichting-Polhausen transition model seem to be the most conservative ones, predicting the lowest performance, however, differences reduce with airfoil thickness. At fully turbulent flow conditions, a lower performance around the design point C_{LDES}=0.8 is expected. Indeed, for the 18% airfoil, performance ranges between 85 and 95, whereas, for the 24% airfoil, performance reduces to 70-80. Nevertheless, performance levels still remain high.

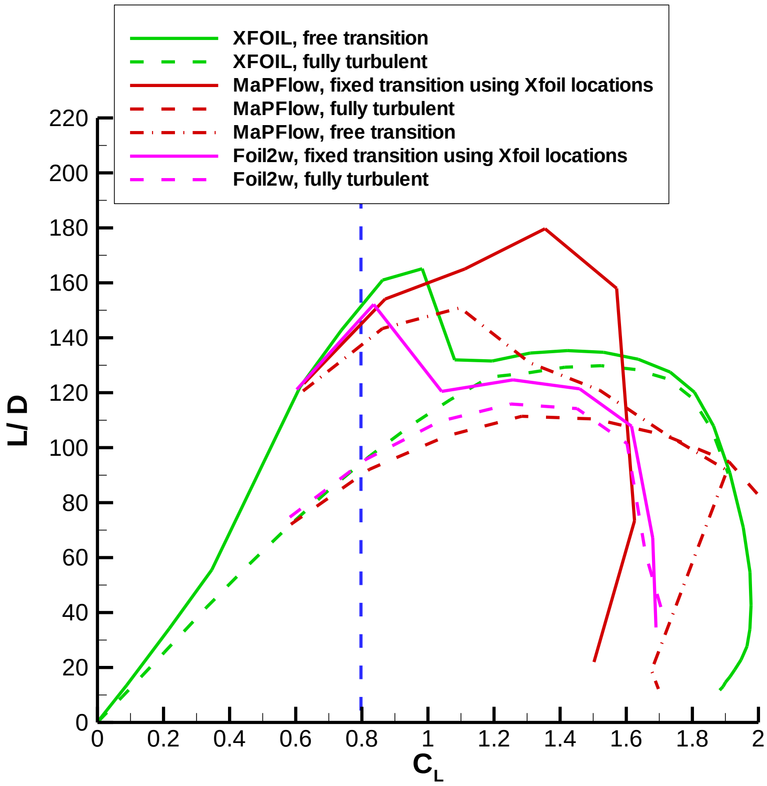

FIGURE 4: Performance (L/D) of the 18% LL 10-90 airfoil for transitional and fully turbulent flow conditions. Comparison among MaPFlow (CFD solver), Foil2w (viscous-inviscid interaction solver) and XFOIL calculations. Fixed transition locations were taken from XFOIL using the e^N model with N=4.

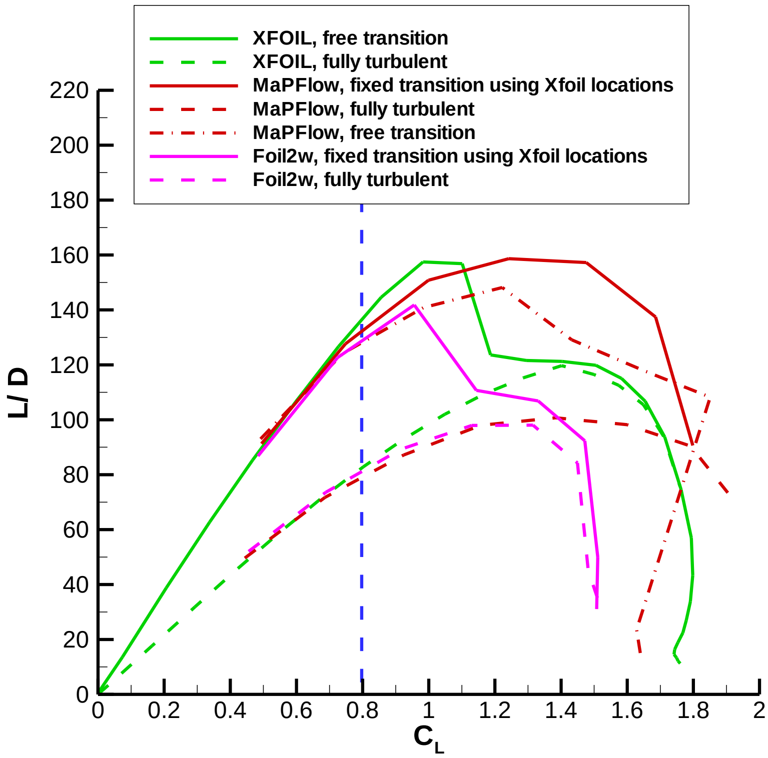

FIGURE 5: Performance (L/D) of the 24% LL 10-90 airfoil for transitional and fully turbulent flow conditions. Comparison among MaPFlow (CFD solver), Foil2w (viscous-inviscid interaction solver) and XFOIL calculations. Fixed transition locations were taken from XFOIL using the e^N model with N=4.

4. Conclusion

Low lift airfoils were designed by maximizing the performance (L/D) around the design point C_{LDES} =0.8 instead of C_{LDES}=1.2 to1.3 which is the normal range for high lift profiles. In the present work, two airfoil families were designed and evaluated, the first one using a laminar / turbulent weighting equal to 30%-70% and the second one using a laminar / turbulent weighting equal to 10%-90% (or 20%-80% for the thickest airfoils). Preliminary calculations with XFOIL showed that the 10-90 family, although more conservative in terms of performance, exhibits more consistent characteristics as thickness increases, both geometrically and performance wise. Therefore, it was chosen for further evaluation using both a Navier-Stokes and a viscous-inviscid interaction solver. The investigation demonstrated that at transitional flow conditions all models predict considerably high performance values, higher than 100, due to the fact that the design point C_{LDES} =0.8 corresponds to laminar flow. At fully turbulent flow conditions, the performance is significantly reduced as expected, reaching a minimum of 60 for the 30% 20-80 airfoil. These results suggest that the designed low lift family airfoils look promising to be used in LIR blades.

5. Learning objectives

The need for designing suitable low lift airfoil families for large low-induction rotors of reduced power density. How this design is materialized and verified at high Reynolds numbers by means of high fidelity computational tools. Performance expectations for low lift profiles in connection to their relative thickness.

6. References

[1] "New aerodynamics rotor concepts specifically for very large offshore wind turbines", Edited by H.A. Madsen, L. Bergami and F. Rasmussen. INNWIND.EU D2.11 Deliverable, September 2013

[2] P.K. Chaviaropoulos and G. Sieros, "Design of Low Induction Rotors for use in large offshore wind farms", Proc. Scientific Track, EWEA 2014, Barcelona.

[3] Feoktistov, V. "Differential Evolution", Springer Science & Business Media, 2006

[4] Powell, M.J.D. "A view of algorithms for optimization without derivatives", Cambridge University Technical Report DAMTP2007

[5] The XFOIL home page, *http://web.mit.edu/drela/Public/web/XFOIL/*

[6] Papadakis G. and Voutsinas S.G., 2014, "In view of accelerating CFD simulations through coupling with vortex particle approximations" in: *The Science of Making Torque from Wind Journal of Physics: Conference Series*, IOP Publishing Copenhagen pp. 012126

[7] Riziotis V.A. and Voutsinas S.G., 2008, "Dynamic stall modelling on airfoils based on strong viscous–inviscid interaction coupling", *International Journal for Numerical Methods in Fluids* 56 2 185-208.

[8] H. Schlichting , 1968, "Boundary Layer Theory", McGraw-Hill.